Fate of [^{14}C/^{3}H]Emamectin Benzoate in Cabbage. 1. Extractable Residues

Louis S. Crouch,* Christopher L. Wrzesinski, and William F. Feely

Department of Drug Metabolism—Rahway, Pesticide Metabolism and Environmental Safety Group, Merck Research Laboratories, P.O. Box 450, Three Bridges, New Jersey 08887

Cabbage, after treatment with eight weekly applications of the semisynthetic avermectin at a 0.015 lb a.i./acre (1×) or a 5× rate, was collected at preharvest intervals (PHI) from 2 h to 10 d. For foliage at 2 h to 10 d PHI: (1) the total ^{14}C-residue declined from 450 to 200 (1×) or 2900 to 1300 (5×) ppb, (2) the total ^{14}C-residue was 78−92% extractable, (3) the extractable residue consisted of the parent as well as polar and avermectin-like residues, (4) the parent declined from 90 to 7 ppb (1×), and (5) polar residues *in toto* ranged from 120−170 ppb (1×). For the extractable residue, (1) 10 avermectin-like residues were identified with the parent accounting for 4−38% of the total, (2) the polar residues were found to be extremely complex, consisting of many minor components and no apparent conjugates, and (3) the polar residues *in toto* accounted for 23−75% of the total.

Keywords: *Emamectin; MK-0244; avermectin; metabolism; cabbage*

INTRODUCTION

Emamectin benzoate (MK-0244, CAS 137512-74-4, registry numbers provided by the authors) is a mixture of two active compounds: 4″-deoxy-4″-(*epi*-methylamino)avermectin B_{1a} (MAB1A, CAS 121124-29-6) and 4″-deoxy-4″-(*epi*-methylamino)avermectin B_{1b} (MAB1B, CAS 121424-52-0) (Figure 1). These compounds, which are homologous semisynthetic macrolides of approximately 900 molecular weight, are derived from the natural fermentation products avermectin B_{1a} and B_{1b} (from *Streptomyces avermitilis*) by replacement of the 4″-hydroxyl constituent with an *epi*-methylamino group. Avermectin B_{1a+b} is also known as abamectin, avermectin B_1, or MK-0936. Abamectin is registered worldwide for use as a miticide or insecticide on a variety of crops. The avermectin homologues in emamectin benzoate are specified as a ratio greater than 9 B_{1a}:1 B_{1b}. Emamectin benzoate is formulated as a benzoate salt due to the amine constituent at the 4″ position. Emamectin benzoate is an effective larvacide against lepidoptera (Trumble et al., 1987) and is being developed for use on leafy vegetables, cole crops, and fruiting vegetables as well as other crops.

The isolation of residues from the surface of cabbage treated with a single application of emamectin benzoate and identification of residue components by NMR and MS has previously been reported (Wrzesinski et al., 1996). The fate of emamectin benzoate has also been studied in lettuce (Crouch and Feely, 1995), rats (Mushtaq et al., 1996), and goats (Mushtaq et al., 1997). In this and the accompanying paper (Feely and Crouch, 1997), the identification and characterization of the components of the extractable and unextractable residues from cabbage treated with multiple applications of [^{14}C]MAB1A benzoate to simulate actual field usage of emamectin benzoate are reported. Therefore, the residues described in these reports would be expected to be the same as those in the diet of humans and animals consuming emamectin-treated crops. In this report, the extractable residues from cabbage treated at the field usage rate for emamectin benzoate and a 5× exaggerated rate and harvested at 2 h to 10 days after the last application were examined by a screening HPLC method to quantify the major components of the residue. More extensive procedures were then used to identify or characterize the extractable residue components from plants treated at the exaggerated rate and harvested at 3 days after the last application, including (1) serial HPLC cochromatography with standards, (2) attempts to identify sugar conjugates, and (3) quantitation of total intact macrocycle by fluorescent derivatization. Also, the use of [^{3}H/^{14}C]MAB1A benzoate at the last application allowed the fate of a single application to be followed.

MATERIALS AND METHODS

Test Compounds and Reference Standards. The test compounds used in this study ([^{14}C]MAB1A benzoate and [^{3}H]-MAB1A) were supplied by the Labeled Compound Synthesis Group, Department of Drug Metabolism, Merck Research Laboratories, Rahway, NJ. The MAB1A homologue was chosen since it is the major homologue, comprising ≥90% of emamectin benzoate. Little or no difference in degradation would be expected between these homologues, which differ only by a single methylene group on an aliphatic side chain (Figure 1). For example, metabolism studies of the homologues of the similar compound ivermectin indicated no differences within four animal species (Chiu et al., 1987); the metabolism of the emamectin homologues was similar in rat liver slices (Crouch, L. S., unpublished results), and the photodegradation of the emamectin homologues on glass resulted in the same rate of degradation as well as formation of homologous degradates (Wrzesinski, C. L., unpublished results). The [^{14}C]MAB1A benzoate was labeled at one of five positions (C3, C7, C11, C13, or C23) per MAB1A molecule (Figure 1) at a specific activity (sp. act.) of 29.0 μCi/mg. The distribution of the label between the five positions in [^{14}C]MAB1A was equal. The [^{3}H]MAB1A (labeled at 5 H, Figure 1) had a sp. act. of 11.88 mCi/mg as the free base. The solutions of ^{14}C-test compounds for the first seven applications were made by dissolving [^{14}C]MAB1A in a vehicle consisting of a proprietary agricultural formulation (blank emulsifiable concentrate, EC) that was then diluted with water to 60 ppm (1×) or 300 ppm (5×) shortly before application. The ^{14}C-test compounds for the last (eighth) application were formulated in vehicle as for the first seven

* Author to whom correspondence should be addressed [fax (908) 369-8811; e-mail louis_crouch@merck.com].

S0021-8561(96)00908-9 CCC: $14.00

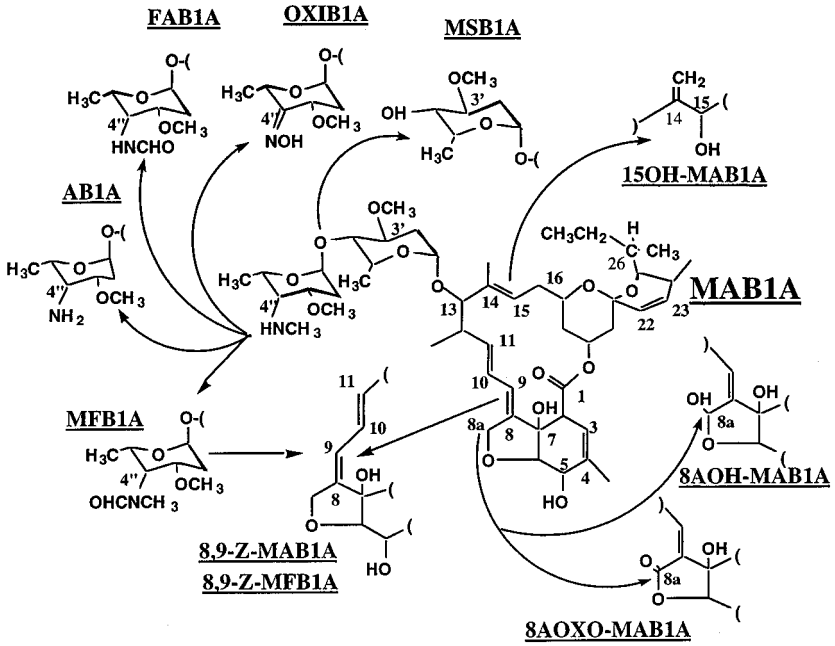

Figure 1. Structure of MAB1A and degradates. Radiolabeled positions of MAB1A were C-3, -7, -11, -13 and -23 for ^{14}C and H-5 for ^{3}H. Emamectin benzoate (MK-0244) is the salt of a mixture of the "a" (shown) and "b" avermectin homologues. The "b" homologue (MAB1B) has a methyl substituent at C-26 rather than ethyl as indicated for the "a" homologue. The ratio MAB1A:MAB1B in emamectin benzoate is greater than 9.

applications except that ^{3}H-MAB1A was added so that the sp. act. for both radionuclides was nominally 29.0 μCi/mg of MAB1A benzoate. HPLC analysis of all test compounds and application solutions indicated 95−99% radiopurity.

The following avermectin standards were obtained from Merck Research Laboratories, Three Bridges or Rahway, NJ: avermectin B_{1a} monosaccharide (MSB1A, CAS 71831−09−9), 4″-deoxy-4″-*epi*-*N*-formylavermectin B_1 (FAB1, CAS 169265-45-6), 4″-deoxy-4″-*epi*-*N*-formyl-4″-*epi*-*N*-methylavermectin B_1 (MFB1, CAS 169265-46-7), [^{14}C]-4″-deoxy-4″-(hydroxyimino)-avermectin B_{1a} (OXIB1A, CAS 172102-46-4), [^{14}C]-(8,9-*Z*)-4″-deoxy-4″-*epi*-*N*-formyl-4″-*epi*-N-methylavermectin B_{1a} (8,9-Z-MFB1A, CAS 172275-65-9), 8a-oxo-4″-deoxy-4″-(*epi*-methylamino)avermectin B_1 (8AOXO-MAB1), 8a-hydroxy-4″-deoxy-4″-(*epi*-methylamino)avermectin B_1 (8AOH-MAB1), 4″-deoxy-4″-*epi*-aminoavermectin B_1 (AB1, CAS 121064-68-4), emamectin benzoate (MAB1), and (8,9-*Z*)-4″-deoxy-4″-(*epi*-methylamino)avermectin B_{1a} (8,9-Z-MAB1A, CAS 169529-95-7) (Figure 1). The avermectin standards either contained only the respective B_{1a} homologue (MSB1A, 8,9-Z-MAB1A, 8,9-Z-MFB1A) or, for FAB1, MFB1, 8AOXO-MAB1, 8AOH-MAB1, AB1, and MAB1, consisted nearly entirely of the respective B_{1a} homologue (FAB1A, MFB1A, 8AOXO-MAB1A, 8AOH-MAB1A, AB1A, MAB1A) with a minor amount of the respective B_{1b} homologue.

Cabbage Cultivation, Treatment, and Harvest. The field phase of the study was conducted in a 30 ft × 60 ft test plot shelter at ABC Laboratories, Inc., Columbia, MO. Each plot consisted of an approximately 3 ft × 8 ft × 24 in. deep oblong, steel stock tank. The tanks were buried 18 in. into the ground and were filled with 18 in. of soil (sandy loam). The shelter was covered with corrugated Filon fiberglass to allow light transmittance, but the panels directly above the plots were removed to allow full sunlight to reach the test plots. A Copenhagen Market variety of cabbage seed was germinated, and seedlings were transplanted into plots on April 24, 1991. Portable shields of plastic film were used to prevent precipitation from reaching the plots and were in place when it rained during the daytime and nightly between approximately 5 pm and 7 am local time. The plots were irrigated with deionized water applied to the soil at regular intervals during the study.

Seven weekly applications of [^{14}C]MAB1A benzoate were made to the 1× and 5× plots; the first application was made on April 30, 1991. The application rates were 0.015 lb a.i./acre (1× plot) and 0.075 lb a.i./acre (5× plot). The eighth application to the 1× and 5× plots using [^{3}H/^{14}C]MAB1A benzoate was made on June 18, 1991. The applications were made using a CO_2-powered handheld sprayer with a total volume of 52 mL of spray solution applied per application. A third plot consisted of untreated plants to serve as controls.

At harvest, each plot contained approximately 21 mature, healthy plants, and the foliage completely covered the plot soil. Cabbage was harvested at 2 h, 1 day, 3 days, 7 days, and 10 days following the final application. At each PHI three or six cabbage plants were harvested from each plot. The harvested plants were divided into three specimen types: dead leaf, consisting of necrotic or partially necrotic tissue still attached to the plants, roots, and foliage or raw agricultural commodity. The foliage consisted of the combined cabbage wrapper leaf and head except for 3 plants each from the 5× plot at 3 and 7 days PHI, for which the wrapper leaf and head were collected as separate specimens. All specimens were frozen soon after harvest.

Specimen Processing and Extraction. The frozen foliage specimens were minced in a Hobart Model 84186 food cutter, and subsamples were homogenized on ice with approximately 2 mL of methanol per gram of specimen using a Brinkmann Model 10/35 Polytron. The frozen dead leaf specimens were thawed, minced with scissors, and then homogenized on ice with about 3−7 mL of methanol per gram of specimen using a Brinkmann Model 10/35 Polytron. The frozen root specimens were thawed and rinsed thoroughly with water. The rinsed root specimens were minced with scissors and then homogenized in a Waring blender with methanol.

Aliquots of the foliage methanol homogenates of each individual specimen from the 1× and 5× plots, each containing about 1−2 g wet weight, were extracted serially with methanol followed by 1:1 methanol/water, each containing ammonium acetate (1 or 5 mM), as previously described (Crouch and Feely, 1995). The extracts from individual foliage specimens from the 1× and 5× plots were then analyzed by HPLC. The foliage methanol homogenates from three plants from the 5× plot at each PHI, each containing 80−320 g wet weight, were composited and extracted by the same procedure. The extracts from the composited foliage specimens were then used in serial chromatographic procedures including HPLC analysis. The foliage marcs, which remained after the extraction of the composited foliage specimens, were dried and saved for de-

termination of unextractable radioactivity. Root and dead leaf methanol homogenates were not extracted.

Quantitation of Radioactivity. Liquid scintillation counting (LSC) of extractable residues was performed with a Packard Model 4530, 460, 460M, or 2500 TR liquid scintillation counter with Packard Insta-Gel XF as fluor. Radiocombustion analysis (RCA) was used for determination of the total radioactivity in the foliage methanol homogenates and marcs. For RCA, oxidation of samples was performed using Packard Model B306 or 307 sample oxidizers dispensing Monophase S (Packard) for ^3H_2O quantitation and Carbosorb (Packard) plus Permafluor V (Packard) for $^{14}CO_2$ quantitation by LSC.

Solid-Phase Extraction of Extractable Residues. The extractable residues from the composited homogenates of foliage from the 5× plots were fractionated by solid-phase extraction using C18 columns. Briefly, a series of columns (Mega Bond-Elut C18, 6 cm^3; Varian) were conditioned by rinsing with 10−20 mL of methanol followed by 10−20 mL of water and were equilibrated with 10−20 mL of 70:30 methanol:water. A solution of extractable residues in 70:30 methanol:water (5−25 mL) was applied to each column, and the eluates were collected. The columns were then eluted with 5−50 mL of 70% methanol containing ammonium acetate (5 mM), and the eluates were combined with the loading eluates. These combined eluates comprised the "total polar residues" (TPR) fraction. The columns were then eluted with 5−20 mL of methanol containing ammonium acetate (5 mM), and these eluates comprised the "avermectin-like residues" (AVM) fraction. For some analyses the total polar residues were subfractionated by solid-phase extraction. For this subfractionation, the C18 columns were conditioned by rinsing with water. Aliquots of the extractable residues from the composited homogenates of foliage from the 5× plots in water were applied to the columns. The columns were rinsed with water followed by 25% methanol containing ammonium acetate (5 mM), and these eluates comprised the "unretained polar residues" (UPR) fraction. Next, the columns were rinsed with 70% methanol containing ammonium acetate (5 mM), and these eluates comprised the "retained polar residues" (RPR) fraction. Finally, the columns were washed with methanol containing ammonium acetate (5 mM), and these eluates comprised the AVM fraction as for the first solid-phase extraction procedure. The equivalent fractions of extractable residues from untreated plants were also obtained by the same procedures for the purpose of background subtraction in certain assays. See Figure 2A for a summary of the relationships between the subfractions in the solid-phase extraction procedures.

HPLC Equipment and Methods. Five HPLC systems were used and consisted of the following instrumentation: System 1, Hewlett-Packard 1040A diode array detector, Hewlett-Packard 1040M data station and Spectra-Physics SP8800 solvent delivery system; system 2, Hewlett-Packard 1040A diode array detector, Hewlett-Packard 85B data station, and Spectra-Physics SP8700 solvent delivery system; system 3, Spectra-Physics SP 8480XR variable-wavelength detector, Perkin-Elmer data station, and Perkin-Elmer 250 solvent delivery system; system 4, LDC Spectromonitor III (Model 1204A) variable-wavelength detector, Hewlett-Packard 3394A integrator, and Spectra-Physics SP8700 solvent delivery system; system 5, two Hewlett-Packard 1040A diode array detectors with optical upgrades, one Hewlett-Packard ChemStation data station and Spectra-Physics SP8800 and 8700 solvent delivery systems. All five HPLC systems were also equipped with a Rheodyne 7125 injector and a Pharmacia Frac-100 fraction collector.

The HPLC methods used in the study are listed in Table 1. Analyses were performed on the following samples using the HPLC methods indicated: application solutions (method 1), extractable residues from foliage of individual 1× and 5× plants (method 2), and the TPR fraction from foliage of 5× plants, 3 days PHI (method 7). A multistep (serial) HPLC analysis was performed on the AVM fraction from the extractable residue of the composited foliage from 5× plants, 3 days PHI. This multistep HPLC analysis in general consisted of three steps using methods of differing selectivity (methods 3, 4, and 5 or 6) and was used to confirm the identity of residue

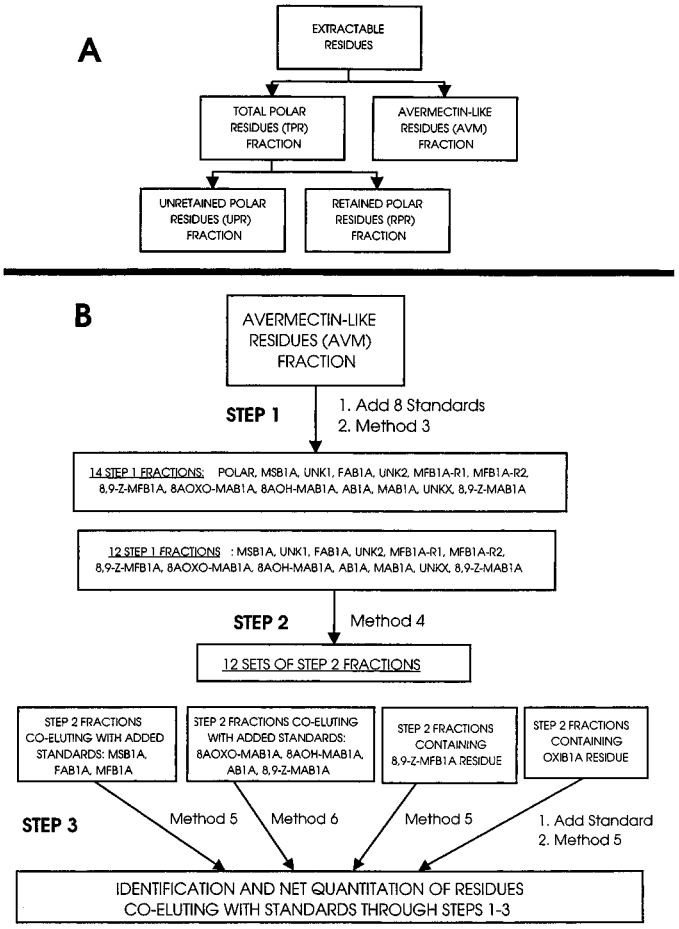

Figure 2. Solid-phase extraction and multistep HPLC analysis of extractable residues from composited foliage. (A) Relationship of various fractions obtained by solid phase extraction. (B) General multistep HPLC analysis; additional HPLC steps (not shown) were necessary for some residues. See Materials and Methods for details of procedures.

components (see Figure 2B). For the multistep HPLC analysis, the AVM residue fraction was first mixed with eight standards: MSB1A, FAB1, MFB1, 8AOH-MAB1, 8AOXO-MAB1, AB1, MAB1, and 8,9-Z-MAB1A. The mixture was then subjected to the first HPLC step (method 3) from which 14 fractions were obtained. These 14 fractions were designated, according to elution with the respective "a" homologue of the standards where applicable, as polar, MSB1A, UNK 1, FAB1A, UNK 2, MFB1A R1 (early-eluting rotamer), MFB1A R2 (late-eluting rotamer), 8,9-Z-MFB1A, 8AOXO-MAB1A, 8AOH-MAB1A, AB1A, MAB1A, UNK X, and 8,9-Z-MAB1A. Method 4 was used as the second step of the multistep HPLC analysis for all 14 fractions from method 3 with the exception of the polar fraction. Certain method 4 eluate fractions from each run were then selected for the third HPLC step (method 5 or 6) if they contained residues that coeluted with a standard or a significant unknown residue. The [^{14}C]OXIB1A standard was added to the method 4 fraction containing that residue prior to the third HPLC step, whereas [^{14}C]-8,9-Z-MFB1A was used as an external standard for comparison to the residue. The HPLC methods used for other sample types are given with the specific procedures described below.

Fluorescence Derivatization of Polar Extractable Residues. The RPR fractions from composited foliage of 5× plants and untreated plants as well as avermectin standards were derivatized using reagents and solvents as previously described (Prabhu et al., 1991). Briefly, the solvent used was CH_3CN, and the dehydration of the avermectin dihydroxycyclohexene ring to the fluorescent derivative was effected with trifluoroacetic anhydride (TFAA) using *N*-methylimidazole (NMIM) as a catalyst. A nominal ratio of 18 CH_3CN:1 NMIM:1 TFAA was used. Prior to derivatization, all samples were

Table 1. HPLC Methods

no.	column supplier	column type	solvent A	solvent B	time (min)	% B
1	Axxiom	Axxichrom C18	water (5 mM AA[a])	methanol (5 mM AA)	0	80
					45	90
					50	100
					60	100
2	Axxiom	Axxichrom C18	water (5 mM AA)	methanol (5 mM AA)	0	85
					35	85
					50	100
					60	100
3	Axxiom	Axxichrom C18	water (5 mM AA)	methanol (5 mM AA)	0	85
					45	87
					65	100
					70	100
4	Shiseido	Dychrom C18	water (0.4 mM TEA[b])	acetonitrile (0.4 mM TEA)	0	55
					15	55
					45	80
					55	100
					60	100
5	E. Merck	Lichrospher diol	isooctane (0.4 mM TEA)	ethanol (0.4 mM TEA)	0	6.5
					20	6.5
					35	15
					60	15
6	E. Merck	Lichrospher diol	isooctane (0.4 mM TEA)	ethanol (0.4 mM TEA)	0	10
					30	10
					45	22.5
					55	22.5
7	Phenomenex	C18	water (5 mM AA)	methanol (5 mM AA)	0	0
					10	0
					65	100
					75	100
8	Metachem	Inertsil C8	water (5 mM AA)	methanol (5 mM AA)	0	25
					10	25
					10.1	100
					30	100
9	Axxiom	Axxichrom C18	water (5 mM AA)	methanol (5 mM AA)	0	25
					10	25
					50	100
					60	100

[a] Ammonium acetate or [b]triethylamine used as modifiers. For all methods eluent gradient changes were linear between indicated time points. For all methods but method 3 the flow rate was 1 mL/min and the column dimensions were 4.6 × 250 mm. For method 3, the flow rate was 3 mL/min and the column dimensions were 9 × 250 mm. For all methods except method 8 the eluate was monitored by diode array detection between approximately 200 and 400 or 600 nm. For method 8, the eluate fluorescence was monitored at 475 nm with excitation = 365 nm.

dried under N_2 in glass tubes with addition of CH_3CN during drying as appropriate to facilitate evaporation of water. Samples were assayed before and after derivatization by HPLC method 8 (Table 1), and 1 mL fractions of eluate were collected as appropriate for LSC assay. The eluate fluorescence was monitored at excitation and emission wavelengths of 365 and 475 nm, receptively (10 nm slits). Eluate fluorescence was determined using a Perkin-Elmer LS-50B spectrofluorometer with an LC flow cell accessory. To quantify fluorescence by HPLC method 8 the total peak area between 800 and 1800 s (13.3−30 min) was used. To correct for fluorescence contribution from natural products, a linear standard curve of fluorescence peak area versus wet weight equivalents (0.2−2.0 g) for the corresponding derivatized RPR fraction from untreated plants was constructed (not shown). The fluorescence from natural products after derivatization of untreated cabbage was then subtracted from the appropriate derivatized polar residues samples on a wet weight equivalents basis using this standard curve.

Enzymatic Treatments of Polar Extractable Residues. The TPR fraction from the composited foliage of 5× plants was subjected separately to hydrolysis with α- and β-glucosidase. For incubation with β-glucosidase, 5 mL of sodium acetate buffer (100 mM, pH 5.0) was added to two flasks, each containing a dried aliquot of the TPR fraction, and to an empty flask. Approximately 25 mg (5.6 U/mg, 140 units total) of β-glucosidase (Sigma, isolated from almonds) was then added to each of these three flasks. Finally, approximately 20 mg of salicin (2-(hydroxymethyl)phenyl β-D-glucopyranoside, Sigma) was added to the flask with no TPR fraction and to one flask containing the TPR fraction. For incubation with α-glucosidase 5 mL of sodium phosphate buffer (100 mM, pH 6.8) was added to two flasks, each containing a dried aliquot of the TPR fraction, and to an empty flask. Approximately 25 mg (4.5 U/mg, 112.5 U total) of α-glucosidase (Sigma, Type 1) was then added to each of these three flasks. Finally, approximately 2 mg of *p*-nitrophenyl α-D-glucopyranoside (Sigma) was added to one flask containing the TPR fraction and to the flask with no TPR fraction. All six flasks were then incubated for approximately 24 h at 37 °C. After 24 h, 5 mL of methanol was added to each flask, and the flasks were vortexed. Aliquots of the supernatants from the flasks were then analyzed for total radioactivity and by HPLC method 9. Salicin and its hydrolysis product 2-(hydroxymethyl)phenol (Sigma), *p*-nitrophenyl α-D-glucopyranoside and its hydrolysis product *p*-nitrophenol (Sigma), and the TPR fraction prior to hydrolysis were also analyzed by HPLC method 8 (Table 1).

Acid Treatment of Polar Extractable Residues. The TPR fraction from the composited foliage of 5× plants was subjected to an acid hydrolysis procedure similar to that used to hydrolyze natural avermectins to monosaccharide and aglycon derivatives (Mrozik et al., 1982). For the acid hydrolysis, 20 mg of MK-0244 was weighed in a 25 mL glass vial, and 4 mL of tetrahydrofuran (THF) was added. To a second 25 mL glass vial approximately 0.14 μg of [^{14}C]MAB1A equivalents of the TPR fraction was added and dried, and 4 mL of tetrahydrofuran (THF) was added. Next, a solution of 50% H_2SO_4 (18 M H_3O^+) in water was prepared, and 1.8 mL was added to each of the THF solutions, giving a total volume of 5.8 mL and a concentration of 5.6 M H_3O^+. Both solutions were stirred at room temperature for approximately 24 h. An aliquot (25 mL) of the hydrolyzed MK-0244 solution was assayed by HPLC method 1. The hydrolyzed polar residue solution was neutralized with a concentrated NaOH solution,

Table 2. Total and Extractable ^{14}C-Residue of Cabbage Foliage[a]

		residue fraction		
phi	rate	total	extractable	unextractable
2 h	1×, %[b]	100	83.7 (2.0)	16.3 (2.0)
	5×, %	100	91.1 (0.7)	8.9 (0.7)
	1×, ppb[c]	453 (142)	379	74
	5×, ppb	2889 (305)	2632	257
1 day	1×, %	100	83.3 (3.7)	16.7 (3.7)
	5×, %	100	85.8 (3.2)	14.2 (3.2)
	1×, ppb	379 (112)	316	63
	5×, ppb	2471 (1416)	2120	351
3 days	1×, %	100	82.8 (3.5)	17.2 (3.5)
	5×, %	100	86.4 (4.0)	13.6 (4.0)
	1×, ppb	296 (105)	245	51
	5×, ppb	1887 (745)	1630	257
7 days	1×, %	100	82.6 (2.8)	17.4 (2.8)
	5×, %	100	81.4 (3.1)	18.6 (3.1)
	1×, ppb	264 (51)	218	46
	5×, ppb	1241 (634)	1010	231
10 days	1×, %	100	78.5 (7.0)	21.5 (7.0)
	5×, %	100	83.4 (2.9)	16.6 (2.9)
	1×, ppb	198 (37)	155	43
	5×, ppb	1275 (597)	1063	212

[a] The foliage from each of 3 or 6 plants per PHI and rate was analyzed for total ^{14}C-residue and extracted individually. Total ^{14}C-residue and unextractable residue were determined by RCA and extractable residue by LSC. [b] Mean and (standard deviation) of ^{14}C-radioactivity recovered from extraction. [c] Mean and (standard deviation) of concentration of total residue or residue fraction as ppb MAB1A benzoate equivalents. Recovery of radioactivity from extractions ranged between 83% and 101%. Limit of detection was 2 ppb for RCA.

and aliquots were taken for radioactivity determination (50 mL) and analysis (1 mL) by HPLC method 1 (Table 1).

RESULTS

Distribution of Radioactivity in Plants. The distribution of ^{14}C-radioactivity between foliage, dead leaf, and roots in plants from either the 1× or 5× plots was similar and did not appear to change significantly with PHI. The foliage (about 80%), dead leaf (about 20%), and roots (less than 2%) accounted for the indicated proportions of the total plant ^{14}C-radioactivity at either rate (data not shown). When the foliage from the 5× plants was divided into head leaf and wrapper leaf, greater than 90% of the ^{14}C-radioactivity in the foliage was found in the wrapper leaf (data not shown). Therefore, discarding the cabbage wrapper leaf before consumption would greatly reduce exposure to emamectin residues. The distribution of ^{3}H-radioactivity in the plants from either the 1× or 5× plots was greater than 95% in the foliage at 2 h PHI, declining to about 90% at 10 days with the balance accounted for in the dead leaf; no ^{3}H-radioactivity was found in roots (data not shown).

Quantitation of Total and Extractable Residue in Foliage. The mean total ^{14}C-residue in plants from the 1× plot declined steadily from 453 ppb parent ([^{14}C]-MAB1A benzoate) equivalents at 2 h to 198 ppb at 10 days (Table 2). The mean total ^{14}C-residue in plants from the 5× plot declined steadily from 2889 ppb at 2 h to 1275 ppb at 10 days and was approximately 4−7-fold of the 1× plants at each PHI (Table 2). When the foliage of plants from the 5× plot was separated into wrapper leaf and head leaf the mean total ^{14}C-residue was 2693 and 132 ppb, respectively, at 3 days PHI and 3397 and 99 ppb, respectively, at 7 days PHI (data not shown). The decline in mean total ^{14}C-residue in the 1× and 5× plants relative to the 2 h PHI was comparable at the 1 day PHI through 10 days (Figure 3). However, although the mean foliage wet weight relative to the 2 h PHI in general increased, this increase did not appear to account for the total ^{14}C-residue decline in the 1× or 5× plants (Figure 3). The mean extractable residue of foliage from the 1× plants was relatively constant with PHI at approximately 78−84% of the [^{14}C]-TTR, whereas for the 5× plants appeared to decline slightly from approximately 91% at 2 h PHI to approximately 83% at 10 days (Table 2). In the 1× plants, the mean concentration of extractable residue decreased from 379 to 155 ppb and unextractable residue from 74 to 43 ppb from 2 h to 10 days PHI (Table 2). In the 5× plants, the mean concentration of extractable residue decreased from 2632 to 1063 ppb; however, the unextractable residue increased slightly from 2 h (257 ppb) to 1 day (351 ppb) PHI and then declined steadily thereafter to 212 ppb by 10 days PHI (Table 2).

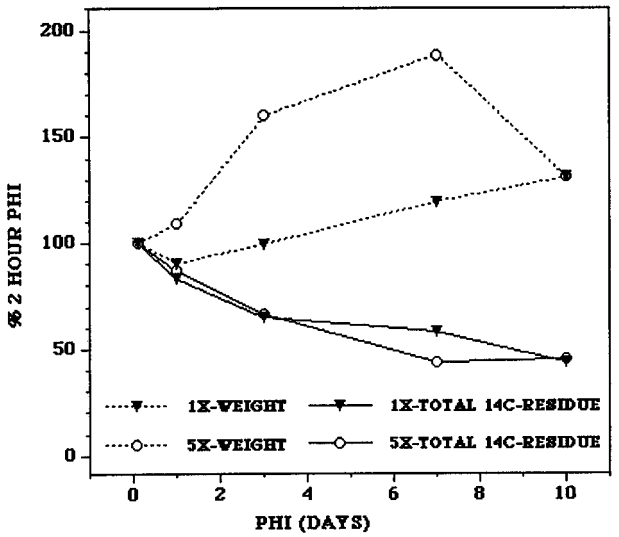

Figure 3. Relation of cabbage foliage wet weight and total ^{14}C-residue. The mean wet weight of cabbage foliage and the mean total ^{14}C-residue for three or six plants per PHI were expressed as percent of the respective values at the first PHI (2 h).

The total ^{3}H-residue of cabbage foliage could not quantified accurately as parent equivalents due to the unknown amounts of ^{14}C-residues on each plant at the time of the [^{3}H]MAB1A benzoate application. The extractable ^{3}H-residue was determined for foliage composited from three plants for each PHI and rate and ranged from 96−98% at 2 h to 89−90% at 10 days.

Quantitation of Extractable Residue Components from Foliage by Single-Step HPLC Analysis. The extractable residue was obtained from the foliage of individual plants, and standards were added for analysis by a single-step HPLC method (method 2, Table 1). This method was useful to rapidly assess the major identified individual residues (MAB1A, MFB1A, and 8,9-Z-MAB1A) and for quantitation of the major residue fraction (polar) for foliage from all individual plants in the study. However, as will be discussed in a subsequent section, a true assessment of the complex MAB1A residue as well as confirmation of the identity of individual residues required a multistep HPLC analysis. Although the multistep HPLC analysis demonstrated that the single-step HPLC analysis significantly overestimated and/or did not completely resolve the identified residue components, it was not practical to apply the more complex method (Figure 2B) on a routine basis.

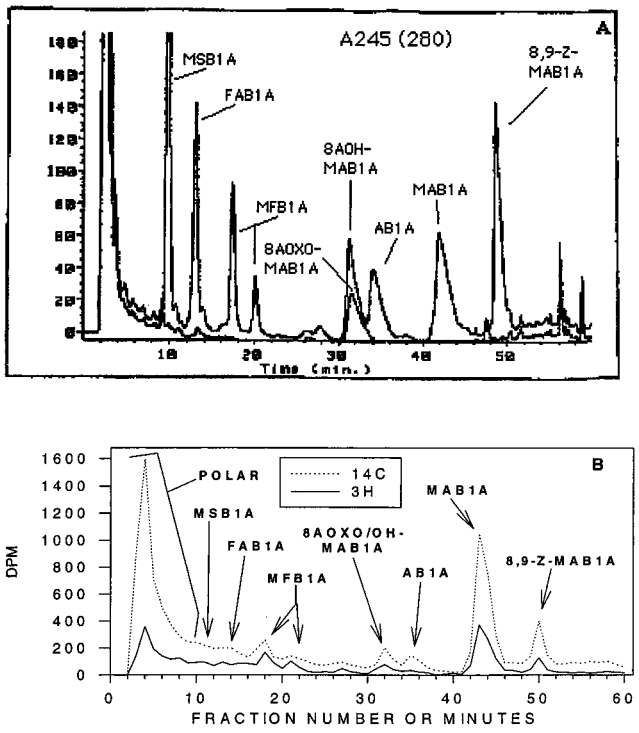

Figure 4. Example analysis of extractable residue from foliage of a single 5× plant with added standards (MSB1A, FAB1, MFB1, 8AOH-MAB1, 8AOXO-MAB1, AB1A, MAB1A, and 8,9-Z-MAB1A) by the single-step HPLC method (method 2, Table 1) used for screening all individual plants. See Tables 3 and 4 for a summary of analysis results. (A) UV profile at 245 nm (280 nm for 8AOXO-MAB1A) with "a" homologues of standards (Figure 1) indicated. (B) Radioprofile with residues corresponding to added standards or polar residues (all residues eluting before MSB1A) indicated. Undefined residues (Tables 3 and 4) are those not corresponding to either polar residues or added standards and are quantified as an aggregate.

For the single-step HPLC analysis eight component fractions of the extractable residue (polar, MSB1A, FAB1A, MFB1A, 8AOXO/OH-MAB1A, AB1A, MAB1A, and 8,9-Z-MAB1A) were quantified. The UV profile (the UV absorbance of residues is entirely from the added standards) and the ^{14}C- and ^{3}H-radioprofiles obtained for the extractable residue from a 5× plant (3 days PHI) are shown in Figure 4. The "a" homologues of the 8AOH-MAB1 and 8AOH-MAB1 standards (Figure 1) coeluted but all other standards were resolved. The "a" homologue of the MFB1 standard (Figure 1) can be seen as a pair of rotamers eluting as a major and a minor peak at approximately 18−20 min (Figure 4A). The rotamers result from hindered rotation of the 4″-(*N*-formylamino) group (Figure 1). Peaks of radioactivity (Figure 4B) corresponding to the UV peaks of all added standards (Figure 4A) can be seen. The radioactivity corresponding to the polar residues was defined as the sum of all radioactivity eluting before the MSB1A standard (Figure 4). The undefined radioactivity was the sum of radioactivity in all eluate fractions not coeluting with a UV peak or eluting as polar residues before the MSB1A standard (Figure 4).

The parent [^{14}C]MAB1A was a mean of approximately 38% of the extractable radioactivity at 2 h PHI in the 5× plants and exhibited a rapid decline thereafter to approximately 10% by 7−10 days PHI (Table 3). There appeared to be an effect of application rate on the extent of MAB1A breakdown, as the [^{14}C]MAB1A in the 5× plants was consistently a higher percentage of the eluted ^{14}C-radioactivity than in the 1× plants. In the 1× plants, the parent [^{14}C]MAB1A was only approximately 22% at 2 h PHI, declining to approximately 4% by 10 days (Table 3). Also, the polar ^{14}C-residues were lower in the 5× plants as compared to the 1× plants, increasing from about 42% of the total extractable ^{14}C-residue at 2 h PHI to about 75% by 10 days in the 1× plants but from approximately 23% to 53% over the same period for the 5× plants (Table 3). The remaining ^{14}C-residue components (MSB1A, FAB1A, MFB1A, 8AOH-MAB1A, 8AOXO-MAB1A, AB1A, and 8,9-Z-MAB1A) were in general higher in the 5× plants than the 1× plants at each PHI (Table 3). However, with the exception of the MFB1A residue at 2 h (1× and 5× plants) and 1 day PHI (5× plants), no defined residue component except the polar residues and MAB1A exceeded 10% of the total eluted ^{14}C-radioactivity at any PHI (Table 3). The ^{3}H-MAB1A residue was approximately 60% of the extractable ^{3}H-radioactivity at 2 h PHI in the 5× plants and declined to about 8−11% by 7−10 days PHI (Table 4). As with the extractable ^{14}C-residues (Table 3), there appeared to be an effect of application rate on the extent of MAB1A breakdown since [^{3}H]MAB1A in the 1× plants was only about 37% of the extractable ^{3}H-radioactivity at 2 h PHI and declined to 3% by 10 days, whereas for the 5× plants it declined from about 59% at 2 h to 11% by 10 days PHI (Table 4). Also, as for the polar ^{14}C-residues (Table 3), the polar ^{3}H-residues were always higher in the 1× plants than the 5× plants, increasing from about 14% of the total extractable ^{3}H-residue at 2 h PHI to 83% by 10 days in the 1× plants versus about 4% to 54% over the same period for the 5× plants (Table 4). Furthermore, the remaining ^{3}H-residue components (MSB1A, FAB1A, MFB1A, 8AOH-MAB1A, 8AOXO-MAB1A, AB1A, and 8,9-Z-MAB1A) were in general higher in the 5× plants than the 1× plants at each PHI (Table 4) as also occurred with ^{14}C-residues (Table 3). With the exception of the MFB1A residue at 2 h (1× and 5× plants), 1 day and 3 days (5× plants) PHI, no defined residue component except the polar residues and MAB1A exceeded 10% of the total extractable ^{3}H-radioactivity at any PHI (Table 4). Overall, the four major components of the extractable residues from cabbage foliage were the polar residues, MFB1A, MAB1A, and 8,9-Z-MAB1A (Tables 3 and 4). Interestingly, the undefined residues were overall rather similar among PHIs and rates, ranging between 6 and 20% of the extractable ^{14}C- and ^{3}H-residues with most values at approximately 10% of the extractable residue.

The concentrations of each of the ^{14}C-residue components in cabbage foliage as estimated by the single-step HPLC method are summarized in Table 3. For the 1× plants, the polar ^{14}C-residues were fairly constant at 150−170 ppb from 2 h to 7 days PHI and then declined to 116 ppb by 10 days. For the 5× plants, the ^{14}C-polar residues increased from a mean of about 600 ppb at 2 h PHI to 800 ppb by 3 days and then declined to about 300−600 ppb at 7−10 days. For either the 1× or 5× plants the parent [^{14}C]MAB1A decreased sharply by about 50% from 2 h to 1 day PHI, from 998 to 490 ppb (5×) or 86 to 42 ppb (1×). After 1 day PHI, [^{14}C]MAB1A declined more slowly, to about 100 ppb (5×) or 10 ppb (1×) by 10 days PHI. The [^{14}C]-MFB1A residue in the 5× plants was fairly constant at about 300 ppb from 2 h to 1 day PHI and then declined to about 40−60 ppb by 7−10 days, while in the 1× plants it declined steadily from about 40 to 5 ppb from 2 h to 10 days. The [^{14}C]-8,9-Z-MAB1A residue decreased steadily in the 1×

Table 3. Single-Step HPLC Analyses of Extractable ^{14}C-Residue of Cabbage Foliage[a]

residue component	rate	2 h	1 day	3 days	7 days	10 days
POLAR	1×, %[b]	41.8 (6.1)	51.5 (6.3)	64.1 (5.9)	70.9 (4.7)	74.5 (5.2)
	5×, %	*23.0 (5.1)*	*32.4 (5.3)*	*40.5 (4.1)*	*55.8 (5.6)*	*53.1 (3.3)*
	1×, ppb[c]	157 (47)	167 (72)	154 (51)	154 (28)	116 (26)
	5×, ppb	*603 (147)*	*648 (315)*	*806 (218)*	*388 (173)*	*557 (229)*
MSB1A	1×, %	2.0 (0.5)	3.7 (0.9)	2.6 (0.6)	2.2 (0.4)	2.2 (0.2)
	5×, %	*3.2 (0.5)*	*3.2 (0.6)*	*4.3 (0.8)*	*3.9 (0.3)*	*3.6 (0.1)*
	1×, ppb	7 (3)	11 (3)	7 (3)	5 (2)	4 (1)
	5×, ppb	*86 (20)*	*64 (31)*	*84 (17)*	*28 (15)*	*38 (17)*
FAB1A	1×, %	3.0 (0.8)	2.7 (0.3)	2.4 (0.4)	2.2 (0.3)	2.4 (0.3)
	5×, %	*10.5 (0.2)*	*14.9 (1.2)*	*9.3 (0.1)*	*5.2 (0.3)*	*5.7 (1.2)*
	1×, ppb	11 (4)	9 (4)	6 (2)	5 (1)	4 (2)
	5×, ppb	*108 (14)*	*156 (81)*	*132 (60)*	*34 (19)*	*57 (33)*
MFB1A	1×, %	10.1 (4.5)	5.2 (0.5)	3.9 (0.8)	2.9 (0.4)	2.9 (0.8)
	5×, %	*10.5 (0.2)*	*14.9 (1.2)*	*9.3 (0.1)*	*5.2 (0.3)*	*5.7 (1.2)*
	1×, ppb	41 (28)	17 (5)	10 (5)	7 (2)	5 (3)
	5×, ppb	*276 (44)*	*327 (211)*	*187 (61)*	*37 (19)*	*64 (42)*
8AOXO/OH-MAB1A	1×, %	3.4 (2.2)	1.9 (0.1)	1.1 (0.3)	0.9 (0.1)	0.6 (0.2)
	5×, %	*2.3 (1.1)*	*3.0 (0.4)*	*2.1 (0.9)*	*1.5 (1.1)*	*1.5 (0.4)*
	1×, ppb	14 (12)	6 (2)	2 (1)	2 (1)	1 (0)
	5×, ppb	*62 (33)*	*61 (34)*	*47 (37)*	*13 (14)*	*17 (11)*
AB1A	1×, %	2.2 (0.4)	1.7 (0.2)	1.6 (0.5)	1.2 (0.3)	1.0 (0.3)
	5×, %	*2.5 (0.7)*	*2.3 (0.7)*	*3.2 (0.3)*	*1.7 (0.3)*	*2.6 (0.4)*
	1×, ppb	8 (4)	6 (2)	4 (3)	3 (1)	2 (1)
	5×, ppb	*65 (13)*	*51 (32)*	*65 (19)*	*11 (4)*	*28 (16)*
MAB1A	1×	22.3 (4.5)	13.3 (1.1)	8.8 (2.9)	6.4 (2.2)	4.1 (1.7)
	5×	*37.9 (4.5)*	*21.2 (4.8)*	*16.6 (2.8)*	*10.5 (3.2)*	*10.4 (0.9)*
	1×, ppb	86 (38)	42 (11)	23 (12)	14 (6)	7 (3)
	5×, ppb	*998 (173)*	*490 (362)*	*344 (166)*	*77 (57)*	*111 (56)*
8,9-Z-MAB1A	1×	4.4 (0.8)	4.1 (0.7)	3.1 (0.7)	2.7 (0.8)	2.3 (0.5)
	5×	*6.2 (0.6)*	*5.4 (1.3)*	*6.3 (0.9)*	*4.0 (0.7)*	*4.6 (0.1)*
	1×, ppb	17 (8)	13 (4)	8 (4)	6 (3)	4 (2)
	5×, ppb	*163 (20)*	*125 (96)*	*129 (56)*	*29 (17)*	*49 (23)*
undefined[d]	1×	10.7 (4.1)	15.9 (3.4)	12.3 (1.5)	10.7 (1.0)	10.1 (2.0)
	5×	*10.2 (0.9)*	*9.9 (1.2)*	*11.3 (0.6)*	*12.6 (1.8)*	*13.4 (0.9)*
	1×, ppb	39 (16)	49 (14)	31 (14)	23 (5)	16 (7)
	5×, ppb	*270 (49)*	*210 (120)*	*225 (64)*	*85 (35)*	*140 (60)*

[a] Values are mean and (standard deviation) for individual assays of extractable residues from each of three to six plants per rate and PHI by HPLC method 2. Assignments of residue components as indicated in Figure 4. Recoveries from each analysis (calculated from radioactivity in extractable residue sample prior to drying and reconstituting for HPLC analysis) averaged approximately 70% for 1× plants and 83% for 5× plants. [b] Percent of radioactivity recovered from HPLC column. [c] ppb as ^{14}C-MAB1A benzoate equivalents. [d] Sum of all radioactivity not coeluting with added standards or corresponding to polar residues.

Table 4. Single-Step HPLC Analyses of Extractable ^{3}H-Residue of Cabbage Foliage[a]

		% eluted radioactivity (SD)				
residue component	rate	2 h	1 day	3 days	7 days	10 days
polar	1×	14.3 (3.3)	40.4 (8.9)	64.6 (6.2)	77.1 (9.0)	82.9 (5.4)
	5×	4.0 (1.8)	11.7 (3.1)	25.4 (3.5)	58.9 (11.0)	53.6 (13.3)
MSB1A	1×	2.1 (1.0)	3.7 (1.2)	2.7 (.07)	2.1 (0.6)	2.4 (1.0)
	5×	1.2 (0.6)	4.5 (4.0)	4.5 (0.2)	5.6 (2.8)	3.4 (0.2)
FAB1A	1×	4.5 (1.5)	3.5 (1.1)	2.8 (0.9)	1.9 (0.8)	1.8 (1.1)
	5×	3.0 (0.3)	10.5 (2.2)	8.7 (1.6)	3.3 (2.8)	5.5 (0.7)
MFB1A	1×	15.1 (4.6)	7.5 (1.6)	4.8 (1.7)	2.1 (1.0)	1.0 (0.4)
	5×	15.4 (2.1)	28.0 (3.8)	15.1 (0.9)	6.8 (3.1)	4.5 (3.5)
8AOXO/OH-MAB1A	1×	6.0 (2.6)	2.6 (0.7)	1.7 (0.5)	0.7 (0.4)	0.5 (0.5)
	5×	2.1 (1.4)	3.6 (0.8)	3.4 (0.6)	1.7 (1.5)	1.8 (0.9)
AB1A	1×	3.0 (0.6)	2.4 (1.4)	1.8 (1.3)	0.7 (0.5)	0.6 (0.1)
	5×	2.3 (1.1)	2.0 (1.2)	3.2 (0.6)	2.1 (3.0)	2.3 (1.6)
MAB1A	1×	37.3 (5.4)	17.2 (3.3)	8.1 (1.8)	6.1 (3.1)	3.0 (2.1)
	5×	59.3 (3.7)	25.2 (9.0)	19.7 (4.1)	7.5 (5.5)	10.9 (0.3)
8,9-Z-MAB1A	1×	5.5 (0.5)	2.6 (1.1)	2.1 (0.6)	1.7 (0.5)	1.3 (0.9)
	5×	4.9 (0.4)	3.9 (1.1)	6.2 (0.8)	3.0 (2.8)	4.0 (0.9)
undefined[b]	1×	12.4 (6.0)	19.4 (7.1)	11.4 (1.8)	7.4 (3.2)	6.5 (2.4)
	5×	7.8 (2.1)	10.6 (2.4)	13.7 (4.3)	11.1 (1.7)	13.9 (7.6)

[a] Values are mean and (standard deviation) for individual assays of extractable residues from each of three to six plants per rate and PHI by HPLC method 2. Assignments of residue components as indicated in Figure 4. Recoveries from each analysis (calculated from radioactivity in extractable residue sample prior to drying and reconstituting for HPLC analysis) averaged approximately 66% for 1× plants and 91% for 5× plants. [b] Sum of all radioactivity not coeluting with added standards or corresponding to polar residues.

plants from 17 to 4 ppb, but in the 5× plants the decline was more erratic, from 163 ppb at 2 h to 49 ppb by 10 days. For the remaining residue components (MSB1A, FAB1A, 8AOXO/OH-MAB1A, and AB1A), the concentrations followed a similar pattern throughout the harvest period, declining from 8−14 ppb to 1−4 ppb from 2 h to 10 days in the 1× plants and from 62−100 ppb to 17−38 ppb in the 5× plants (Table 3).

Identification and Characterization of Extractable Residues from Foliage by Multistep HPLC Analysis. The AVM fraction of extractable residue from composited 5× plants (3 days PHI) was spiked with

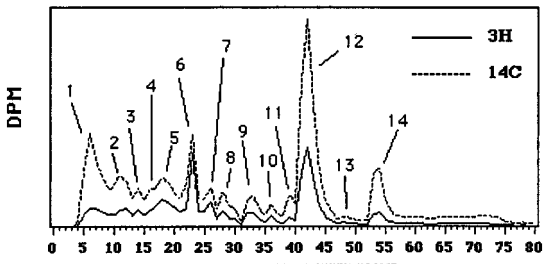

NO.	RESIDUE	FRACTIONS
1	POLAR	1-13
2	MSB1A	14
3	UNK 1	15-16
4	FAB1A	17
5	UNK 2	18-21
6	MFB1A R1	22-23
7	MFB1A R2	25-26
8	8,9-Z-MFB1A	28-30
9	8AOXO-MAB1A	32-33
10	8AOH-MAB1A	36-37
11	AB1A	38-39
12	MAB1A	41-43
13	UNK X	47-49
14	8,9-Z-MAB1A	53-54

Figure 5. Step 1 of multistep HPLC analysis of extractable residue from cabbage foliage. The AVM fraction (Figure 2) from composited foliage of 5× plants was mixed with eight standards (MSB1A, FAB1, MFB1, 8AOH-MAB1, 8AOXO-MAB1, AB1A, MAB1A, and 8,9-Z-MAB1A), fractionated by method 3, and 14 crude fractions were obtained by pooling eluate fractions as indicated. Nine of the crude fractions (2, 4, 6, 7, 9, 10, 11, 12, 14) were pooled according to coelution with the "a" homologue of the added standards (not shown). Fraction 8 was assumed to contain 8,9-Z-MFB1A on the basis of its elution relative to MFB1A (not shown). All but two of the 14 fractions (polar, UNK X) were then refractionated by the second step of the multistep HPLC analysis (method 4; see Figure 6).

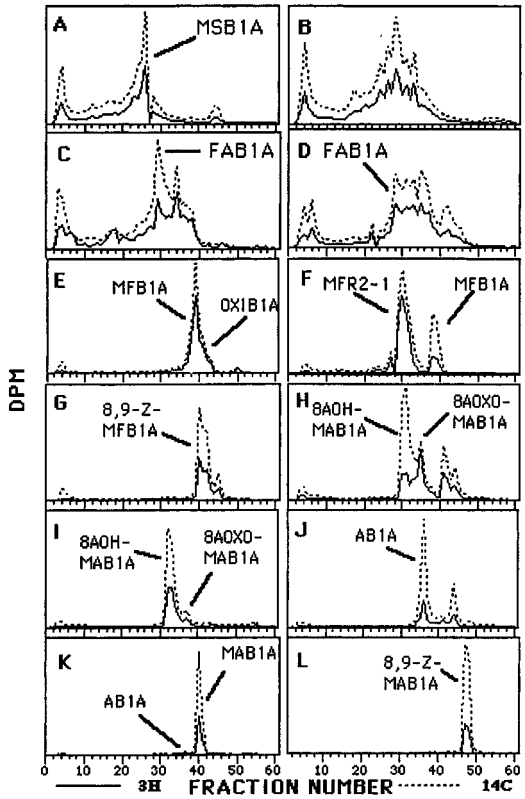

Figure 6. Step 2 of multistep HPLC analysis of extractable residue from cabbage foliage. Crude fractions (2, 3, 4, 5, 6, 7, 8, 9, 10, 11, 12, 14) from step 1 of the serial HPLC analysis (Figure 5) were rechromatographed by HPLC method 4: (A) 2 = MSB1A; (B) 3 = UNK 1; (C) 4 = FAB1A; (D) 5 = UNK 2 containing some FAB1A; (E) 6 = MFB1A R1; (F) 7 = MFB1A R2; (G) 8 = 8,9-Z-MFB1A; (H) 9 = 8AOXO-MAB1A; (I) 10 = 8AOH-MAB1A; (J) 11 = AB1A; (K) 12 = MAB1A; (L) 14 = 8,9-Z-MAB1A. Standards added before step 1 (Figure 6) coeluted with radioactivity peaks indicated in step 2 for MSB1A, FAB1A, MFB1A, 8AOXO-MAB1A, 8AOH-MAB1A, AB1A, MAB1A, and 8,9-Z-MAB1A (not shown). The OXIB1A and 8,9-Z-MFB1A residues were assumed on the basis of retention times of external standards (not shown). MFR2-1 in F is an unknown residue.

a mixture of standards (MSB1A, FAB1, MFB1, 8AOH-MAB1, 8AOXO-MAB1, AB1, MAB1, and 8,9-Z-MAB1A) and resolved by the first step (method 3, Table 1) of the multistep HPLC analysis (Figure 2B). Fourteen crude fractions of residues were then obtained by pooling eluate fractions according to whether they contained a coeluting standard (not shown) or any significant peaks of unknown radioactive residues (Figure 5). Fraction 8 was assumed to contain the 8,9-Z-MFB1A residue based on its elution relative to the late-eluting MFB1A rotamer (MFB1A R2) (Figure 5). With the exception of the UNK X (lost during workup) and polar (assayed by a different method, not shown) fractions, each of the 14 crude fractions from the first HPLC step was then rechromatographed in the second step (method 4, Table 1) of the multistep HPLC procedure (Figure 6). Coelution with the standards (not shown) added prior to the first serial HPLC step was observed for the MSB1A (Figure 6A), FAB1A (Figure 6C,D), MFB1A (Figure 6E,F), 8AOXO-MAB1A (Figure 6H,I), 8AOH-MAB1A (Figure 6H,I), AB1A (Figure 6J,K), MAB1A (Figure 6K), and 8,9-Z-MAB1A residues (Figure 6L). The identification of the OXIB1A (Figure 6E) and 8,9-Z-MFB1A (Figure 6G) residues was based on retention times of external standards (not shown). The unknown MFR2-1 residue appeared to be the major constituent of the crude MFB1A R2 fraction (Figure 6F). The UNK 1 fraction was resolved into at least eight residue peaks by the second HPLC step (Figure 6B), including ones approximately corresponding to MSB1A (Figure 6A) and FAB1A (Figure 6C). In general, the four early-eluting fractions from the first serial HPLC step (MSB1A, UNK 1, FAB1A, and UNK 2) were the most complex (Figure 6A−D). All fractions of eluate from the second HPLC step corresponding to external (OXIB1A and 8,9-Z-MFB1A) or internal (MSB1A, FAB1A, MFB1, 8AOXO-MAB1A, 8AOH-MAB1A, AB1A, MAB1A, and 8,9-Z-MAB1A) standards were then rechromatographed by the third step of the HPLC analysis (method 5 or 6, Table 1). Coelution of the respective "a" homologues of the internal standards added before the first HPLC step with apparent single residues in the third HPLC step was observed for MSB1A, MFB1A, and FAB1A (method 5, Table 1) and 8AOXO-MAB1A, 8AOH-MAB1A, AB1A, MAB1A, and 8,9-Z-MAB1A (method 6, Table 1) (Table 5). The eluate fractions from the second HPLC step containing the tentatively identified OXIB1A (Figure 6E) were further purified by HPLC (not shown) and then were mixed with the ^{14}C-OXIB1A standard. When the mixture of OXIB1A residue and standard was chromatographed in the third serial HPLC step (method 6, Table 1), coelution of the UV (Figure 7A) and ^{14}C-radioactivity of the standard (Figure 7B) with the ^{3}H- and ^{14}C-radioactivity (Figure 7B) of the OXIB1A residue was observed. Separate analyses of the [^{3}H/^{14}C]-8,9-Z-MFB1A residue from the second HPLC step (Figure 6G) and the [^{14}C]-8,9-Z-MFB1A standard by HPLC method 6 (Table 1) indicated that the retention times of the UV peaks of the standard (Figure 8A) matched those of the radioactivity peaks of the residue (Figure 8B). In addition, unknown residues were still apparent after the

Table 5. Final Identification of Individual Residues by Multistep HPLC Method[a]

residue	method[b]	retention time: standard[c] (t_R, min)	retention time: peak[d] (t_R, fractions)
MSB1A	5	28.9	29,30
FAB1A	5	39.0	39−41
MFB1A[e]	5	29.0, 38.5	29−30, 39−40
OXIB1A[f]	6	37.1	37−38
8,9-Z-MFB1A[e,g]	5	13.0, 18.5	13−14, 18−20
8AOH-MAB1A	6	45.3	46−48
8AOXO-MAB1A	6	36.4	36−38
AB1A	6	51.7	52−55
MAB1A	6	39.5	40−41
8,9-Z-MAB1A	6	28.3	29−31

[a] Retention times of the added or external standards and the peaks of residue radioactivity are summarized for the last step of the multistep HPLC method (Figure 2) for the extractable residues from the composited foliage from 5× plants, 3 days PHI. [b] HPLC method (Table 1) for third step. [c] Retention time of UV peak of standard. [d] Fractions containing peak(s) of residue radioactivity. [e] Retention times refer to rotamer pair. [f] See also Figure 7. [g] See also Figure 8.

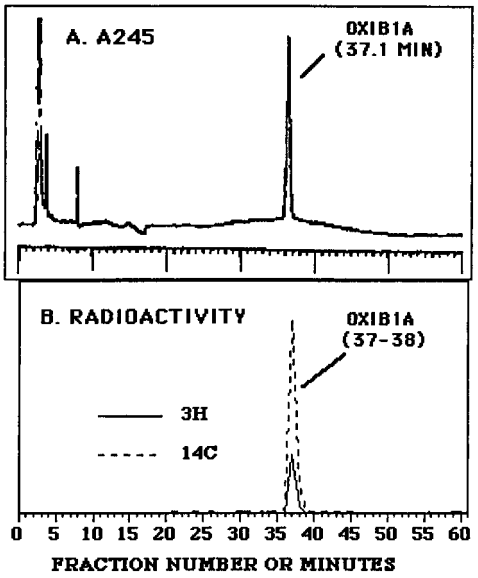

Figure 7. Step 3 of multistep HPLC analysis of extractable residue from cabbage foliage for OXIB1A. The OXIB1A fraction from step 2 of the multistep HPLC analysis (Figure 6E) was partially purified by additional HPLC (not shown), mixed with [^{14}C]OXIB1A standard, and chromatographed by HPLC method 6. (A) UV profile at 245 nm. (B) Radioprofile. Note: tritium radioprofile is from OXIB1A residue.

third serial HPLC step for the 8,9-Z-MFB1A residue (Figure 8B, inset). Therefore, the identities of 10 residues (MSB1A, FAB1A, MFB1A, OXIB1A, 8,9-Z-MFB1A, 8AOXO-MAB1A, 8AOH-MAB1A, AB1A, MAB1A, and 8,9-Z-MAB1A) were confirmed by the multistep HPLC analysis. A comparison of the percentage of extractable ^{14}C-radioactivity coeluting with each standard in the multistep HPLC analysis of composited foliage from three 5× plants (Table 6) to the mean for the single-step HPLC analyses of individual foliage specimens for the same plants (Table 3) indicated that, with the exception of MAB1A, all residues were greatly overestimated by the single-step HPLC analyses. Further, no single residue component except MAB1A exceeded 3% of the extractable residue (Table 6) and, therefore, even less of the total residue. The concentration of the identified residues as determined by the multistep HPLC analysis ranged from 3 ppb (MSB1A) to 192 ppb (MAB1A) as compared to <42 ppb (8AOXO-MAB1A or 8AOH-MAB1A) to 334 ppb (MAB1A) by the single-step HPLC analysis (Table 3). However, at 3 days PHI, the concentration of identified residues in cabbage treated at the field usage (1×) rate would be expected to be approximately 1/5 or less of cabbage

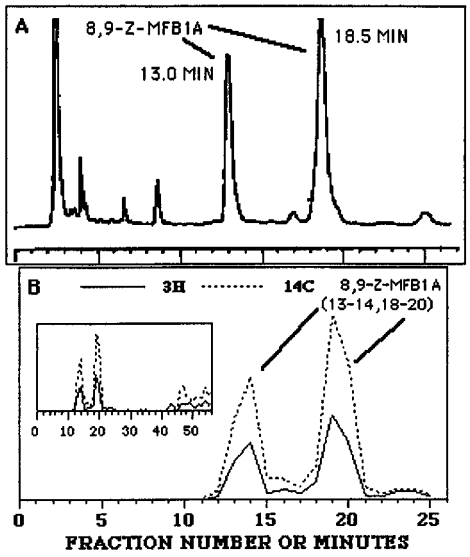

Figure 8. Step 3 of multistep HPLC analysis of extractable residue from cabbage foliage for 8,9-Z-MFB1A. The 8,9-Z-MFB1A fraction from step 2 of the serial HPLC analysis (Figure 6G) and the [^{14}C]-8,9-Z-MFB1A standard were chromatographed separately by HPLC method 6. (A) UV profile of external [^{14}C]-8,9-Z-MFB1A standard at 245 nm. (B) Partial radioprofile of [^{3}H/^{14}C]-8,9-Z-MFB1A residue; inset shows complete radioprofile.

Table 6. Multistep HPLC Analysis of Extractable ^{14}C-Residue of Cabbage Foliage[a]

extractable residue component	%[b]	PPB[c]
MSB1A	0.1	3
FAB1A	0.6	11
MFB1A	1.5	28
OXIB1A	0.2	4
MFR2-1[d]	0.6	11
8,9-Z-MFB1A	0.6	11
8AOXO-MAB1A	0.2	3
8AOH-MAB1A	0.6	11
SUM	0.8	14
AB1A	0.8	15
MAB1A	10.4	192
8,9-Z-MAB1A	2.7	49

[a] Extractable residues from the composited foliage of three 5× plants, 3 days PHI, were subjected to solid-phase extraction [recoveries = 107.4% (^{3}H) and 94.6% (^{14}C)], and the resultant AVM fraction was analyzed by a minimum of three serial HPLC steps (Figure 2). [b] Values are net percentages of total extractable ^{14}C-radioactivity coeluting with standards throughout the procedure for identified residues. [c] ppb as MAB1A benzoate equivalents. [d] Unidentified residue. All values for the multistep HPLC procedure were corrected for recovery at each step. The mean recoveries for the 24 separate HPLC assays performed in the multistep HPLC procedure were 82.7% (^{3}H) and 90.8% (^{14}C).

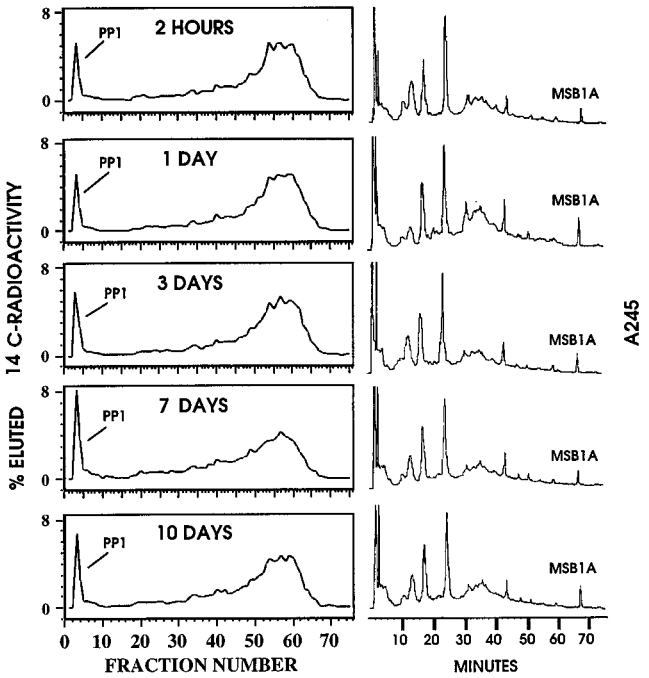

Figure 9. HPLC analysis of polar extractable residues from cabbage foliage. The TPR fraction of extractable residues from composited foliage of three 5× plants at each PHI was mixed with MSB1A standard and analyzed by HPLC method 7 (Table 1). Radioprofiles (left panels) are expressed as percent of total eluted ^{14}C-radioactivity with corresponding UV profiles at 245 nm (right panels). The unretained peak designated PP1 was 9.4% (2 h), 8.9% (1 day), 10.3% (3 days), 14.9% (7 days), and 12.0% (10 days) of the eluted radioactivity at the indicated PHIs or 57 ppb (2 h), 58 ppb (1 day), 83 ppb (3 days), 58 ppb (7 days), and 67 ppb (10 days) MAB1A benzoate equivalents. The MSB1A standard eluted at 67.0 or 67.1 min for each analysis. All other UV peaks are from cabbage natural products. Recovery of radioactivity ranged from 88 to 99%.

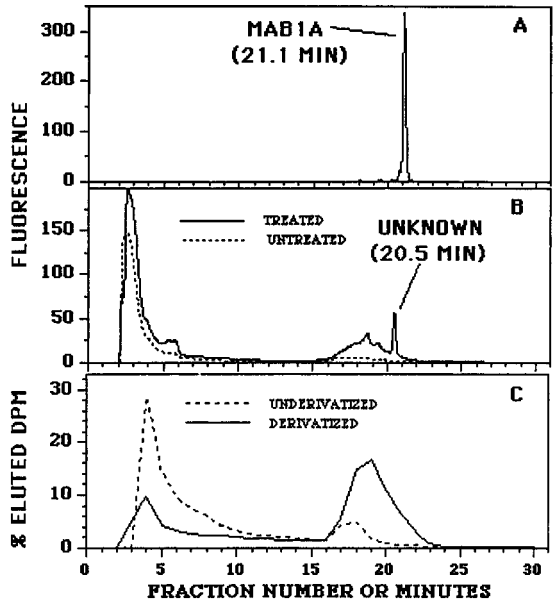

Figure 10. HPLC analysis of RPR fraction of ^{14}C-residues from cabbage foliage before and after derivatization. The RPR fraction of extractable residues from composited foliage of three 5× plants (3 days PHI) and MK-0244 were subjected to fluorescence derivatization. The derivatives of MK-0244 and polar extractable residues as well as underivatized RPR fraction residues were analyzed by HPLC method 8 (Table 1). (A) Fluoroprofile of MK-0244 derivative (0.1 mg). (B) Fluoroprofile of derivatives of residues in the RPR fraction from 1.38 g wet weight of cabbage foliage from treated plants and equivalent fraction from 0.98 g wet weight of foliage from composited untreated plants. (C) Radioprofile (^{14}C) of derivatized residues from the RPR fraction from B and of the corresponding underivatized residues. Recovery of radioactivity ranged from 99 to 100%. The integrated fluorescence from 13.3 to 30 min for the derivatized residues from the RPR fraction B was approximately 16% of that for MK-0244 (A) on a mass ^{14}C-radioequivalents to mass basis.

treated at the 5× exaggerated rate (Table 6) on the basis of the single-step HPLC analyses (Table 3).

Characterization of Polar Extractable Residues. The TPR fraction of the extractable residues from the composited foliage of 5× plants at each PHI was mixed with MSB1A standard and analyzed by HPLC method 7 (Table 1) to determine whether qualitative changes occurred in the radioprofile of the major extractable residue fraction (Table 3) with increasing time after application. The radioprofiles at all PHIs (Figure 9, left panels) were remarkably similar and were characterized by a sharp unretained peak (PP1) and a broad band of retained but unresolved radioactivity. The UV profiles (Figure 9, right panels) were very consistent between analyses with the added MSB1A standard and many natural products eluting as sharp peaks with essentially no variation in retention times. Essentially all radioactivity eluted before MSB1A (67.0−67.1 min) as expected (Figure 9).

The RPR fractions of extractable residues from the composited foliage of 5× plants (3 days PHI) and untreated plants as well as MK-0244 were subjected to the fluorescent derivatization procedure and assayed by HPLC method 8 (Table 1) in order to estimate the portion of residues retaining the parent macrocycle structure. The MAB1A derivative was well retained and eluted as a sharp peak (Figure 10A). The corresponding derivatives of MSB1A and AB1A eluted just prior to MAB1A, also as sharp peaks (data not shown). The fluorescent products in the RPR fraction from 5× plants (3 days PHI) gave a large unretained peak of fluorescence and a wide band of retained fluorescence with some definition including a significant unknown peak (Figure 10B) eluting just before MAB1A (Figure 10A). The fluorescent products in the corresponding RPR fraction from the foliage of untreated plants gave a large unretained peak of fluorescence as for that from the treated plants (Figure 10B). However, although a broad band of retained fluorescence was also observed for the RPR fraction from untreated plants, this retained band was much lower in intensity and had no definition in contrast to that from the treated plants (Figure 10B). After correction of fluorescence contribution from the matrix, the integrated fluorescence area for the RPR fraction from the foliage of 5× plants (3 days PHI) was approximately 16% of MK-0244 on a mass radioequivalents of [^{14}C]MAB1A benzoate to mass of MK-0244 basis. Inspection of the ^{14}C-radioprofile of the fluorescent products in the RPR fraction (Figure 10C) and its accompanying fluoroprofile (Figure 10B) indicated a poor correlation between radioactivity and fluorescence. For example, the unknown peak of fluorescence eluting at 20.5 min (Figure 10B) had no corresponding peak of radioactivity (Figure 10C). The fluorescent derivatization procedure caused a significant change in the ^{14}C-radioprofile of the RPR fraction by increasing the retention of the majority of the residues (Figure 10C). It is likely that this large increase in retention of residues in the RPR fraction after derivatization is the result of esterification of residue hydroxyl groups with the TFAA used in the procedure.

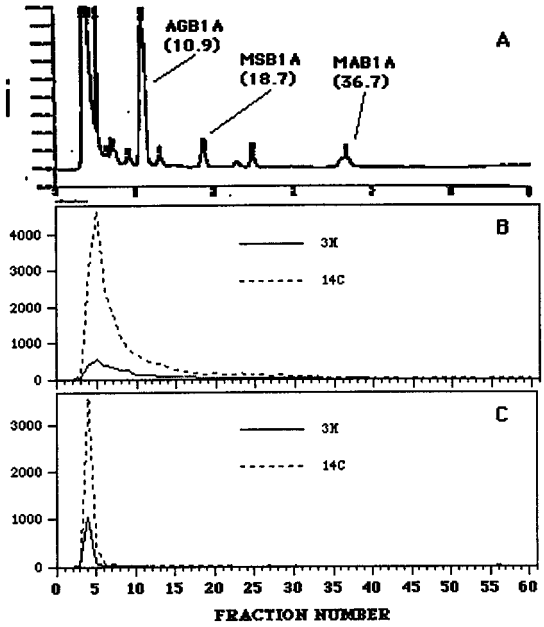

Figure 11. HPLC analysis of polar extractable residues from cabbage foliage after treatment with acid. The TPR fraction of extractable residues from composited foliage of three 5× plants (3 days PHI) and MK-0244 were separately treated with approximately 6 N sulfuric acid for 24 h at room temperature. Each hydrolysate and the TPR fraction before acid treatment were analyzed by HPLC method 1 (Table 1). (A) UV profile (245 nm) of MK-0244 after acid treatment with residual MAB1A and its MSB1A and aglycon (AGB1A) derivatives indicated. (B) Radioprofile of TPR fraction before acid treatment. (C) Radioprofile of TPR fraction after acid treatment. Recovery of radioactivity ranged from 83 to 128%.

The TPR fraction of extractable residues from the composited foliage of 5× plants (3 days PHI) was treated with α-glucosidase or β-glucosidase in the presence or absence of appropriate test substrates (*p*-nitrophenyl α-D-glucopyranoside or salicin, respectively). Analysis of the TPR fraction after these enzymatic hydrolyses by HPLC method 8 (Table 1) revealed that although the test substrates were completely hydrolyzed by their respective enzymes no change indicative of hydrolysis of a residue-glucose conjugate was observed (not shown). Treatment of MK-0244 with approximately 6 N sulfuric acid resulted in nearly complete cleavage of the oleandrose sugars. This was apparent after analysis by HPLC method 1 (Table 1), indicating the appearance of mostly the aglycon derivative (AGB1A) as well as some monosaccharide derivative (MSB1A) with a small amount of residual MAB1A (Figure 11A). Analysis of the TPR fraction before acid treatment by HPLC method 1 gave a broad peak of unretained radioactivity eluting essentially completely before MSB1A (Figure 11A,B), as expected. Analysis of the TPR fraction after acid treatment by HPLC method 1 (Figure 11C) resulted in a narrowing of this peak of unretained radioactivity, and no residues eluting at the retention time of AGB1A or later were seen.

DISCUSSION

The residue in foliage after treatment of cabbage with multiple applications of emamectin benzoate consisted of three parts. (1) The first part was a complex fraction of extractable residues termed avermectin-like, which include MAB1A and degradates closely related in structure. The avermectin-like extractable residues were found to be extremely complex (Figures 5 and 6) and to consist of many minor components plus MAB1A itself rather than a few major components. Nine individual avermectin-like residues (plus MAB1A) were identified by serial HPLC analysis. These residues were MSB1A, FAB1A, MFB1A, 8,9-Z-MFB1A, OXIB1A, 8AOXO-MAB1A, 8AOH-MAB1A, AB1A, and 8,9-Z-MAB1A (Figure 1). These same residues, with the exception of 8AOH-MAB1A and 8AOXO-MAB1A, as well as five additional residues were identified by structural analysis in a previous study using a single application of emamectin benzoate at a higher rate (Wrzesinski et al., 1996). (2) The second part was a complex fraction of extractable residue-termed polar residues whose components are polar relative to the avermectin-like residues on the basis of their elution before MSB1A by RP-HPLC (Figure 4). These polar residues are apparently not conjugates of the parent or residues of similar structure and are likely more highly degraded relative to the parent MAB1A than the identified residues. (3) The third part was the unextractable or bound residue, which mostly appears to represent incorporation of radioactivity into natural products and is the subject of the accompanying paper (Feely and Crouch, 1997).

Role of Photodegradation in the Initial Degradation of Emamectin Benzoate in Cabbage. The results presented in this and the accompanying paper (Feely and Crouch, 1997) indicate that the degradation of MAB1A in cabbage is most likely initially by photodegradation followed by bioincorporation of some of the photoresidues. The MAB1A structure has many possible sites for chemical transformations (Figure 1) and is susceptible to light-induced reactions. When photodegradation of MAB1A as a thin film on glass was studied, approximately 11 major photoproducts were found, including nine primary (one change relative to MAB1A) and two secondary (two changes relative to MAB1A) photodegradates (Feely et al., 1992; Arison, 1991). The nature of the phototransformations included cis−trans isomerization at the 8,9 double bond of MAB1A and two of its primary degradates (FAB1A and AB1A), two oxidations at the 8a position (8AOXO-MAB1A and 8AOH-MAB1A), hydroxylation at the 15 position (15OH-MAB1A), N-demethylation (AB1A), oxidation (to *N*-formyl) or *N*-formylation at the 4″-*N*-methyl group (FAB1A and MFB1A, respectively), loss of the outer oleandrose sugar (MSB1A) (Figure 1), and a double bond shift from the 3,4 to the 2,3 position (δ 2,3 MAB1A, not shown). The major identified residues resulting from photolysis of MAB1A on glass (Feely et al., 1992; Arison, 1991) were also, for the most part, identified as degradates isolated from cabbage. In fact, all of the photodegradates identified after photolysis of MAB1A on glass except for the δ 2,3 rearrangement product, the 8,9-*Z* photoisomers of FAB1A and AB1A and 15OH-MAB1A compound, were found at low levels as MAB1A residues in cabbage (Figure 1, Table 6). The appearance of most of the same MAB1A photodegradates as the major single components of the residue in MK-0244-treated cabbage, therefore, suggests a largely nonmetabolic route for the early stages of MAB1A degradation. The OXIB1A residue (Figure 1) found as a minor degradate in cabbage (Table 6) was not reported as a photodegradate formed on glass. However, since OXIB1A coelutes with MFB1A (Figures 5 and 6) and is formed in minor amounts relative to MFB1A (Table 6) and the nitrogen at the 4″ position has no hydrogen-bearing groups attached (Figure 1), it very possibly

would not been have been detected during purification and subsequent structural analysis of the MFB1A residue formed on glass. It is readily apparent that the primary MAB1A degradates observed as a result of photolysis on cabbage are capable of undergoing additional reactions to a number of secondary, tertiary, or higher products since the demonstrated reactions alone occur as 1−4 reaction types at each of four different sites in the molecule: (1) 4′ (MSB1A), (2) 8,9 (8,9-Z-MAB1A), (3) 8a (8AOH-MAB1A, 8AOXO-MAB1A), and (4) 4″ (FAB1A, MFB1A, OXIB1A and AB1A); see Figure 1. For example, the 8,9-*Z* isomers of the primary MAB1A degradates, FAB1A and AB1A (8,9-Z-FAB1A and 8,9-Z-AB1A) were found as secondary photoproducts in thin films (Feely et al., 1992) and the 8,9-*Z* photoisomers of MSB1A (Wrzesinski et al., 1996) and MFB1A (8,9-Z-MFB1A) were found in cabbage. Since it has been demonstrated that formation of the 8,9-*Z* isomers of MAB1A, MSB1A, and MFB1A occurs on cabbage, it is probable that other cabbage residues with the diene intact, such as FAB1A, 8AOXO-MAB1A, 8AOH-MAB1A, and AB1A (Figure 1), would exist as a pair of geometric isomers at the 8,9 position. The 8,9-*Z* photoisomer of any primary degradate of MAB1A in cabbage, however, would also be susceptible to photooxidative degradation and, therefore, would be found in extremely small amounts since it appears likely that no primary degradate contributes more than 3% to the total extractable residue as demonstrated when a comprehensive HPLC examination of the extractable residue was performed (Table 6). The primary degradates of MAB1A observed in cabbage undergo additional reactions other than photoisomerization at the 8,9 bond. For example, the 8a-oxo and 8a-OH derivatives of MFB1A residues have been found (Wrzesinski et al., 1996). It is clear, then, that as long as MAB1A remains on plant surfaces a large number of minor photodegradates of related structure would probably be present. Although the identified residues from MAB1A degradation in cabbage are most likely produced by photolysis, several of these could also be produced metabolically. The most likely degradates to be formed metabolically are AB1A, a known animal metabolite (Mushtaq et al., 1996, 1997), 8AOXO-MAB1A, formed by soil bacteria (A. Chukwudebe, personal communication), 8AOH-MAB1A, and MSB1A (Figure 1). Less likely potential metabolites would include OXIB1A and FAB1A (Figure 1). Extremely unlikely to have been produced metabolically are 8,9-Z-MFB1A, 8,9-Z-MAB1A, and MFB1A (Figure 1). However, the probability that metabolism of MAB1A in a given crop species would produce all of the same MAB1A degradates that result from photolysis would seem exceedingly low.

The use of [^{3}H/^{14}C]MAB1A for the last application allowed the fate of a single application to be followed. An extremely rapid degradation of [^{3}H]MAB1A from the last application was observed, with only 37.3% (1×) or 59.3% (5×) of the extractable residue consisting of the parent at 2 h PHI. The degradation rate of [^{3}H]MAB1A slowed after the first 2 h, although there was a further decline of about 50% from 2 h to 1 day PHI for the 1× and 5× plants (Table 4). This rapid decline in [^{3}H]-MAB1A is further evidence for photolysis as the mechanism for the initial phase of degradation as the rate is inconsistent with generally slower metabolic transformations. Also, as MAB1A was applied as an aqueous solution, it was most likely confined to the cabbage cuticular surfaces during the first 2 h after application and therefore inaccessible to degradative enzymes. The ratio of carbon 14 to tritium specific activity for the MAB1A used in the last application was approximately 1:1. Inspection of the radioprofiles of residues from the 5× plants at 3 days PHI after the second step of the serial HPLC analysis (Figure 6) reveals that in general the carbon 14 to tritium ratio was greater than 1, which indicates that there these residues remained from the previous application(s) of [^{14}C]MAB1A benzoate. However, for the MFB1A (Figure 6F) and 8AOXO-MAB1A (Figure 6H) residues the isotope ratio was much closer to that of the [^{3}H/^{14}C]MAB1A from the last application. The reason for this is unknown, but it is possible that for these two residues their relative proportions to the other residues were much less in the ^{14}C-residue present on the plants just prior to the ^{3}H/^{14}C-application than in the ^{3}H/^{14}C-residues formed after the ^{3}H/^{14}C-application.

Characterization of Polar Residues. The polar residues were the major fraction of extractable ^{14}C-residues at both rates and at all PHIs except for the 5× plants at 2 h PHI and were present at over 100 ppb in the 1× plants at 3 days PHI and beyond (Table 3). A particular concern for these polar residues would be the presence of any with an intact macrocycle or a macrocycle closely resembling the parent macrocycle (Figure 1) as the avermectin macrocycle is certainly the major determinant of the general toxicity of avermectins. Therefore, the identification and/or characterization of these residues in crops for evaluation of their potential for human toxicity is important.

As the photolysis of MAB1A on glass proved a very useful model for the initial phase of degradation of MAB1A in cabbage to residues of similar structure to the parent (Figure 1) it might also be assumed to be so for the polar MAB1A residues. Continued photolysis of [^{14}C]MAB1A on glass eventually results in total disappearance of MAB1A and residues of related structure and the appearance of unidentified polar residues for which the diene functionality is absent. In addition, an approximate 30% maximal loss of radioactivity results (Wrzesinski, unpublished). Similarly, polar ^{3}H/^{14}C-residues predominated in the extractable residue of cabbage foliage at 7−10 days PHI (Tables 3 and 4), and loss of total ^{14}C-residue was observed over the same period (Table 2, Figure 3). The loss of total ^{14}C-residue in cabbage foliage was apparently not a result of increasing plant mass because although a very similar and smooth decline of total ^{14}C-residue was seen in both treatment groups it was not consistently accompanied by either an increase in plant mass or an increase in plant mass of sufficient magnitude to account for the magnitude of the observed total ^{14}C-residue decline relative to the 2 h PHI (Figure 3). Therefore, loss of total ^{14}C-residue in cabbage could in principle result entirely or in part from photolysis.

The polar residues were analyzed by an HPLC method (method 7, Table 1), which would be expected to retain and potentially resolve them. The TPR fractions from composited foliage from the 5× plants were thus examined over the entire harvest interval, as were the avermectin-like residues by the single-step HPLC method (Tables 3 and 4), to determine whether any significant individual residues occurred. Interestingly, the ^{14}C-radioprofile did not appear to change significantly with PHI, and with the exception of the unretained PP1 peak, no significant individual residues were apparent (Figure 9). As a percentage of the TPR

fraction, PP1 increased slightly from 2 h to 7 days PHI followed by a slight decline by 10 days and as parent equivalents increased from 57 ppb at 2 h to 83 ppb at 3 days followed by a decline to about 60−70 ppb at 7 to 10 days (Figure 9, legend). The lack of retention of the PP1 peak (Figure 9) was suggestive of an avermectin conjugated to a polar moiety. However, no MAB1A or any of its primary degradates (Figure 1) or their respective aglycon or monosaccharide derivatives were released after treatment of the polar residues with acid (Figure 11) or glucosidases (data not shown). These attempted hydrolyses indicated that there were probably no conjugates with glucose on either the disaccharide or macrocycle portions of an avermectin (Figure 1) or with any other polar moieties such as glutathione on the disaccharide portion of an avermectin as one or both oleandrose sugars were cleaved by acid treatment (Figure 11). Furthermore, our laboratory has also demonstrated, by glucose-specific colorimetric assay and/or HPLC analysis, that the residues in the PP1 peak from cabbage (Figure 9) consist of fructose, glucose, and possibly galactose with incorporated radioactivity as well as other discrete but unknown residues. Also, glucose and fructose were identified in the corresponding PP1 fraction from corn foliage by NMR in addition to HPLC and colorimetric assay for glucose (L. Allen, manuscript in preparation). The incorporation of radioactivity into simple sugars likely indicates that the MAB1A macrocycle becomes fragmented to a significant extent prior to bioincorporation during emamectin benzoate degradation in cabbage. Incorporation of radioactivity into simple sugars as a result of MAB1A degradation to macrocycle fragments could easily explain the source of radioactivity for the unextractable residues (Feely and Crouch, 1997), assuming these to be mostly biopolymers whose monomers consist of these sugars or are derived from them. Also, incorporation of radioactivity into sugars would presumably lead to eventual loss of radioactivity via $^{14}CO_2$ and could therefore also account for the observed loss of total ^{14}C-residue (Figure 3) in addition to photolysis as discussed previously. The macrocycle fragments that are precursors for sugars are most likely constituents of the polar residue fraction although none have been isolated and identified at present. That a large and complex compound such as the avermectin MAB1A can be degraded to such an extent to allow incorporation of residues into natural products such as sugars is remarkable. However, incorporation of radioactivity from the similar compound [^{14}C]avermectin B_{1a} into plant natural products such as cellulose or lignin is known (Wislocki et al., 1989; Feely and Wislocki, 1991).

The use of [^{14}C]MAB1A labeled at five positions (C3, C7, C11, C13, or C23) (Figure 1) prevented a facile determination of the origin of the macrocycle fragments that are bioincorporated. However, as the purpose of the study was to determine the fate of as much of the residue as possible and to isolate and identify the major individual residue components, this was most easily achieved by the use of multiply-labeled MAB1A. Also, it must be cautioned that for all unidentified residues, which includes the majority of the polar residues, the reporting of ppb levels as parent equivalents may be an overestimation or underestimation of the actual levels for those residues for which significant fragmentation of the macrocycle occurred, depending on the ratio of labeled to unlabeled carbon positions in the fragments relative to the parent.

The previously discussed results indicated that none of the polar residues were conjugates of MAB1A or its identified degradates, which would be potentially toxic compounds, and that the polar residues consist at least in part of macrocycle fragments, which are unlikely to be toxic. However, it appears that not all polar residues are macrocycle fragments as fluorescent products were observed after derivatization of the RPR fraction (Figures 2, 10B). This is so since the derivatization of avermectins to fluorescent products occurs when the dihydroxy cyclohexene ring at C-2 to C-7 is dehydrated and the resultant aromatic ring is conjugated to the 8,9,10,11 diene (Figure 1). Therefore, it is likely that an intact macrocycle with the diene moiety is present in some of the polar residues. The RPR fraction of extractable residues corresponds approximately to the wide band of retained radioactivity eluting at 10−70 min when the TPR fractions of extractable residues (Figure 2) from composited foliage from 5× plants are assayed by HPLC method 7 (Figure 9) and thus comprises about 90% of the polar residues as the PP1 residue is approximately 10% at each PHI (Figure 9, legend). Therefore, assuming that the RPR fraction of polar residues is approximately 90% of the polar residues at both rates and all PHI (Figure 9, legend), then this fraction would range from about 104 to 186 ppb (1×) or 430 to 725 ppb (5×) in the treatment groups indicated using the results in Table 3 for all PHI. It was estimated that the RPR fraction of extractable residues from the foliage of composted 5× plants at 3 days PHI had approximately 16% of the fluorescence of MK-0244 on a mass radioequivalents of [^{14}C]MAB1A benzoate to mass of MK-0244 basis, which is roughly equivalent to the proportion of polar residues in the RPR fraction possessing an intact macrocycle. Therefore, it follows that if the polar residues with an intact macrocycle in general constitutes about 16% of the RPR fraction this would correspond to about 17−30 ppb (1×) or 69−116 ppb (5×) in the treatment groups indicated. However, the residues in the underivatized RPR fraction are apparently complex as no resolution of peaks of radioactivity was seen (Figure 9). Furthermore, the complexity of the underivatized RPR fraction of extractable residues from cabbage foliage is also apparent after extensive serial HPLC analysis (C. L. Wrzesinski, unpublished results). Also, only one resolved and retained but unknown peak of fluorescence was observed (t_R = 20.5 min) after derivatization of the RPR fraction (Figure 10B), and no resolved and retained peaks of radioactivity were observed, notably none at the retention time of the unknown peak of fluorescence (Figure 10B,C). We have observed that when MK-0244 is photolyzed on glass for 1−8 days and the residues are derivatized that no unretained peak of fluorescence is seen at any time when assayed by HPLC method 7 (L. S. Crouch, unpublished results). Therefore, the unretained peak of fluorescence observed for the derivatives in the RPR fraction (Figure 10B) is probably not due to derivatized residues. This is further substantiated by the presence of a similar unretained peak after derivatization of the corresponding RPR fraction from untreated cabbage (Figure 10B). Therefore, although the subfraction of polar residues containing a macrocycle, and therefore of potential toxicity, may be present up to 30 ppb in the foliage of 1× plants it is likely that they are a multicomponent mixture with each component considerably lower than 30 ppb, thus greatly reducing the potential for toxicity.

Comparative Metabolism of Emamectin Benzoate in Cabbage and Lettuce. Emamectin benzoate metabolism was previously studied in lettuce (Crouch and Feely, 1995) using experimental and analytical procedures very similar to the present study. The results obtained with emamectin benzoate-treated lettuce with regard to the level and decline of total ^{14}C-residue, residue extractability, rapid MAB1A degradation, and profile of identified residues were very close to those presented here for cabbage. In addition, characterization of the polar extractable residues from lettuce indicated that they were chromatographically similar to cabbage (Figure 9) as well as apparently containing no conjugates (Crouch and Feely, 1995) and consisting in part of simple sugars with incorporated radioactivity (L. Allen, manuscript in preparation) as demonstrated for cabbage. The unextractable residues in emamectin-treated lettuce, although not as thoroughly studied as in cabbage (Feely and Crouch, this volume), consisted at least in part of biopolymers such as starch and cellulose as evidenced by [^{14}C]glucose release after acid hydrolysis (Crouch and Feely, 1995). Therefore, the degradation of emamectin benzoate in both cabbage and lettuce is remarkably similar, further supporting the hypothesis that this compound is initially and rapidly photodegraded in plants to complex residues and eventually fragmentation of the avermectin macrocycle occurs, leading to partial incorporation of residues into plant biomolecules.

ABBREVIATIONS USED

AB1, mixture of 4″-deoxy-4″-*epi*-aminoavermectin B_{1a} + B_{1b}; AB1A, 4″-deoxy-4″-*epi*-aminoavermectin B_{1a}; AGB1A, avermectin B_{1a} aglycon; AVM fraction, avermectin-like residues fraction from solid phase extraction of extractable residue; B1A, avermectin B_{1a}; 8AOH-MAB1, mixture of 8a-hydroxy-4″-deoxy-4″-(*epi*-methylamino)avermectin B_{1a} + B_{1b}; 8AOH-MAB1A, 8a-hydroxy-4″-deoxy-4″-(*epi*-methylamino)avermectin B_{1a}; 8AOXO-MAB1, mixture of 8a-oxo-4″-deoxy-4″-(*epi*-methylamino)avermectin B_{1a} + B_{1b}; 8AOXO-MAB1A, 8a-oxo-4″-deoxy-4″-(*epi*-methylamino)avermectin B_{1a}; 8,9-Z-MAB1A, (8,9-*Z*)-4″-deoxy-4″-(*epi*-methylamino)avermectin B_{1a}; 8,9-Z-MFB1A, (8,9-*Z*)-4″-deoxy-4″-*epi*-*N*-formyl-*N*-methylavermectin B_{1a}; FAB1, mixture of 4″-deoxy-4″-*epi*-*N*-formylavermectin B_{1a} + B_{1b}; FAB1A, 4″-deoxy-4″-*epi*-*N*-formylavermectin B_{1a}; 15OH-MAB1A, 14-*exo*-methylene-15-hydroxy-4″-deoxy-4″-(*epi*-methylamino)avermectin B_{1a}; HPLC, high-pressure liquid chromatography; LSC, assay of ^{14}C and/or ^{3}H by liquid scintillation counting technique; MAB1, mixture of 4″-deoxy-4″-(*epi*-methylamino)avermectin B_{1a} + B_{1b}; MAB1A, 4″-deoxy-4″-(*epi*-methylamino)avermectin B_{1a}; MAB1B, 4″-deoxy-4″-(*epi*-methylamino)avermectin B_{1b}; MFB1, mixture of 4″-deoxy-4″-*epi*-*N*-formyl-4″-*epi*-*N*-methylavermectin B_{1a} + B_{1b}; MFB1A, 4″-deoxy-4″-*epi*-*N*-formyl-4″-*epi*-*N*-methylavermectin B_{1a}; MSB1A, avermectin B_{1a} monosaccharide; OXIB1A, 4″-deoxy-4″-(*epi*-hydroxyimino)avermectin B_{1a}; RCA, radiocombustion assay; RPR fraction, retained polar residues fraction from solid-phase extraction of extractable residue; TPR fraction, total polar residues fraction from solid-phase extraction of extractable residue; UPR fraction, unretained polar residues fraction from solid-phase extraction of extractable residue

ACKNOWLEDGMENT

We express our gratitude to ABC Laboratories, and in particular to Eric Feutz, for their excellent horticultural skills and performance of the field phase of this study.

LITERATURE CITED

Arison, B. H. (1991) Merck Internal Memo to L.S. Crouch and W.F. Feely.

Chiu, S.-H. L.; Taub, R.; Sestokas, E.; Lu, A. Y. H.; Jacob, T. A. Comparative In Vivo and In Vitro Metabolism of Ivermectin in Steers, Sheep, Swine and Rat. *Drug Metab. Rev.* **1987**, *18*, 289−302.

Crouch, L. S.; Feely, W. F. Fate of [^{14}C]Emamectin Benzoate in Head Lettuce. *J. Agric. Food Chem.* **1995**, *43*, 75−87.

Feely, W. F.; Wislocki, P. G. Avermectin B_{1a} in Celery: Acetone-Unextractable Residues. *J. Agric. Food Chem.* **1991**, *39*, 963−967.

Feely, W. F.; Crouch, L. S. Fate of [^{14}C]Emamectin Benzoate in Cabbage. 2. Unextractable Residues. *J. Agric. Food Chem.* **1997**, *45*, 2758−2762.

Feely, W. F.; Crouch, L. S.; Arison, B. H.; VandenHeuvel, W. J. A.; Colwell, L. F.; Wislocki, P. G. Photodegradation of 4″-(Epimethylamino)-4″-deoxyavermectin B_{1a} Thin Films on Glass. *J. Agric. Food Chem.* **1992**, *40*, 691−696.

Mrozik, H.; Eskola, P.; Arison, B. H.; Albers-Schönberg, A.; Fisher, M. H. Avermectin Aglycons. *J. Org. Chem.* **1982**, *47*, 489−492.

Mushtaq, M.; Syintsakos, L. R.; Krieter, P. A.; Colletti, A.; Arison, B.; Crouch, L. S.; Wislocki, P. G. Absorption, Tissue Distribution, Excretion, and Metabolism of ^{3}H- and ^{14}C-Labeled Emamectin Benzoate in Rats. *J. Agric. Food Chem.* **1996**, *44*, 3342−3349.

Mushtaq, M.; Syintsakos, L. R.; Crouch, L. S.; Wislocki, P. G. Fate of ^{3}H- and ^{14}C-Labeled Emamectin Benzoate in Lactating Goats. *J. Agric. Food Chem.* **1997**, *45*, 253−259.

Prabhu, S. V.; Wehner, T. A.; Egan, R. S.; Tway, P. T. Determination of 4″-Deoxy-4″-(epimethylamino)avermectin B_1 Benzoate (MK-2044) and Its Delta 8,9-Isomer in Celery and Lettuce by HPLC with Fluorescence Detection. *J. Agric. Food Chem.* **1991**, *39*, 2226−2230.

Trumble, J. T.; Moar, W. J.; Babu, J. R.; Dybas, R. Laboratory Bioassays of the Acute and Antifeedant Effects of Avermectin B1 and a Related Analogue on *Spodoptera Exigua* (Hubner). *J. Agric. Entomol.* **1987**, *4*, 21−28.

Wislocki, P. G.; Grosso, L. S.; Dybas, R. A. Environmental Aspects of Abamectin Use in Crop Protection. In *Ivermectin and Abamectin*; Springer-Verlag: New York, 1989; pp 182−200.

Wrzesinski, C. L.; Arison, B. H.; Smith, J. L.; VandenHeuvel, W. J. A.; Crouch, L. S. Isolation and Identification of Residues of 4"-(epi-Methylamino)-4"-deoxyavermectin B1a Benzoate from the Surface of Cabbage. *J. Agric. Food Chem.* **1996**, *44*, 304−312.

Received for review November 27, 1996. Revised manuscript received April 3, 1997. Accepted April 23, 1997.[⊗]

JF9609082

[⊗] Abstract published in *Advance ACS Abstracts,* June 15, 1997.